Available online at www.sciencedirect.com
ScienceDirect
Journal of Controlled Release 123 (2007) 219–227
journal of controlled release
www.elsevier.com/locate/jconrel

Temperature-sensitive hydrogels with SiO_2–Au nanoshells for controlled drug delivery

Malavosklish Bikram, Andre M. Gobin, Rachel E. Whitmire, Jennifer L. West *

Department of Bioengineering, Rice University, 6100 Main Street, MS 144, Houston, TX, 77005, USA

Received 28 April 2007; accepted 9 August 2007
Available online 19 August 2007

Abstract

Silica–gold (SiO_2–Au) nanoshells are a new class of nanoparticles that consist of a silica dielectric core that is surrounded by a gold shell. These nanoshells are unique because their peak extinctions are very easily tunable over a wide range of wavelengths particularly in the near infrared (IR) region of the spectrum. Light in this region is transmitted through tissue with relatively little attenuation due to absorption. In addition, irradiation of SiO_2–Au nanoshells at their peak extinction coefficient results in the conversion of light to heat energy that produces a local rise in temperature. Thus, to develop a photothermal modulated drug delivery system, we have fabricated nanoshell-composite hydrogels in which SiO_2–Au nanoshells of varying concentrations have been embedded within temperature-sensitive hydrogels, for the purpose of initiating a temperature change with light. *N*-isopropylacrylamide-*co*-acrylamide (NIPAAm-*co*-AAm) hydrogels are temperature-sensitive hydrogels that were fabricated to exhibit a lower critical solution temperature (LCST) slightly above body temperature. The resulting composite hydrogels had the extinction spectrum of the SiO_2–Au nanoshells in which the hydrogels collapsed reversibly in response to temperature (50 °C) and laser irradiation. The degree of collapse of the hydrogels was controlled by the laser fluence as well as the concentration of SiO_2–Au nanoshells. Modulated drug delivery profiles for methylene blue, insulin, and lysozyme were achieved by irradiation of the drug-loaded nanoshell-composite hydrogels, which showed that drug release was dependent upon the molecular weight of the therapeutic molecule.

Keywords: Drug delivery; Nanoparticles; Protein release; Stimuli-sensitive; Controlled

1. Introduction

The lack of control of drug release from conventional drug formulations in response to physiological requirements have led to the development of controlled drug delivery systems [1,2]. In many diseases such as diabetes [3], heart disease [4], and thyroid diseases [5], the administration of a drug is only required at specific time intervals in which constant drug levels could lead to adverse effects. Hence, stimuli-sensitive drug delivery systems were developed to release a drug only in response to metabolic requirements or in the presence of specific stimuli. These environmentally-sensitive delivery systems have been developed to respond to a myriad of stimuli including the presence or absence of specific molecules [6–8], magnetic fields [9,10], ultrasound [11–13], electric fields [14,15], temperature [16–19], pH [20,21], and mechanical forces [22,23].

In addition to these stimuli, light has also been used as a stimulus for modulated drug delivery systems. Light-sensitive hydrogels have been categorized as either UV- or visible light-sensitive hydrogels. UV-sensitive hydrogels have been synthesized by the introduction of bis(4-dimethylamino)phenylmethyl leucocyanide into the polymeric matrix in which ionization of the leuco derivative with UV radiation resulted in discontinuous swelling at a constant temperature [24]. Visible light-sensitive hydrogels have been fabricated by the incorporation of light-sensitive chromophores such as the tri-sodium salt of copper chlorophyllin into poly(*N*-isopropylacrylamide) (NIPAAm) hydrogels in which the absorption of light by the chromophore resulted in the heating and subsequent collapse of the temperature-sensitive hydrogel [25].

Recently, a new class of light-sensitive hydrogels containing optically active metal nanoshells capable of absorbing near

* Corresponding author. Tel.: +1 713 348 5955; fax: +1 713 348 5154.
E-mail address: jwest@rice.edu (J.L. West).

0168-3659/$ - see front matter © 2007 Elsevier B.V. All rights reserved.
doi:10.1016/j.jconrel.2007.08.013

infrared (NIR) light was developed for controlled drug delivery. Sershen et al. incorporated gold–gold sulfide nanoshells into NIPAAm-*co*-acrylamide (AAm) hydrogels in order to initiate a temperature change with light [26]. These nanoshells were designed to absorb light at NIR wavelengths between 800–1200 nm, which can be transmitted through tissue with little attenuation due to the low absorption coefficients of water and hemoglobin on either side of this wavelength window [26]. Therefore, irradiation of the nanoshells within the hydrogel with a laser resulted in the conversion of light to heat energy that produced a reversible volume phase transition in the temperature-sensitive polymeric matrix.

Metal nanoshells are a relatively new class of nanoparticles consisting of a dielectric core nanoparticle surrounded by an ultrathin metal shell. These nanoshells have tunable plasmon resonances that are based on geometric construction [27]. The ratio of shell thickness to core diameter allows nanoshell peak resonance to be tuned while the overall dimensions of the particle allow the relative absorbing and scattering efficiencies to be manipulated [27–29]. Silica–gold (SiO_2–Au) nanoshells are a new class of nanoparticles that have a silica dielectric core, which is surrounded by a gold shell. In contrast to gold–gold sulfide nanoshells, the peak extinction of SiO_2–Au nanoshells are very easily tunable to absorb or scatter light strongly within the wavelengths of 650–900 nm that is commonly known as the NIR region [27]. This region is of significant biological importance and hence nanoshells are currently being investigated for use in the NIR region for a variety of biomedical applications including their use as diagnostic tools [30], contrast enhancements for imaging applications [31,32] and for laser tissue welding [33].

Hydrogels are three-dimensional matrices that have been used to develop many systems for the controlled release of therapeutic proteins [34,35]. Hydrogels based on the thermo-responsive polymer NIPAAm exhibit a lower critical solution temperature (LCST) above which the hydrogel undergoes a reversible volume phase transition at ~32 °C [36,37]. At temperatures below the LCST, the polymer exists in the soluble, expanded form but as the temperature is increased above the LCST, the polymer collapses and precipitates out of solution [38]. However, copolymers of NIPAAm have been prepared in order to alter the hydrophobicity and hence the LCST of NIPAAm. The fabrication of hydrogels consisting of NIPAAm and the hydrophilic monomer AAm results in the formation of hydrogels that have a thin surface layer that facilitates the release of soluble material as the hydrogel collapses above its LCST [36]. In addition, NIPAAm-*co*-AAm hydrogels consisting of 95% NIPAAm and 5% AAm monomers have an LCST of approximately 40 °C [26,39,40].

Therefore, to develop a photothermal modulated drug delivery system in which near IR light of a specific wavelength can be used to induce the collapse of a polymeric matrix loaded with model drug molecules and proteins, we have embedded SiO_2–Au nanoshells of varying concentrations within NIPAAm-*co*-AAm hydrogels. Moreover, these nanoparticles were designed to strongly absorb near IR light at ~808 nm, the emission wavelength of the laser used in these studies. The drug delivery profiles of methylene blue, insulin, and lysozyme were then obtained by photothermal irradiation of the resulting nanoshell-composite hydrogels.

2. Materials and methods

N-isopropylacrylamide (NIPAAm), acrylamide (AAm), *N*,*N*′-methylenebisacrylamide (MBAAm), and phosphorus pentoxide (P_2O_5) were purchased from Aldrich (Milwaukee, Wisconsin). Ammonium persulfate (APS), *N*,*N*,*N*′,*N*′-tetramethylethylenediamine (TEMED), tetrahydrofuran (THF), *n*-hexane was purchased from Sigma (St. Louis, Missouri). Insulin from bovine pancreas (MW 5800), lysozyme (MW 14, 700), β-casein (MW 25, 000), and bovine serum albumin (BSA) (MW 66, 000) were purchased from Sigma (St. Louis, Missouri). Bicinchoninic acid (BCA) protein assay was purchased from Pierce (Rockford, Illinois). Ready gel Tris–HCl gel, 4–15% linear gradient and Bio-rad silver stain plus kit were purchased from Bio-rad (Hercules, CA). EnzChek® lysozyme assay kit was purchased from Invitrogen Molecular Probes (Carlsbad, CA).

2.1. SiO_2–Au nanoshell fabrication

Nanoshells were made as previously described [28]. Briefly, silica cores were grown using the Stöber process, base catalyzed reduction of tetraethyl orthosilicate (Sigma-Aldrich, Milwaukee, WI) in ethanol [41]. The resultant silica nanoparticles were sized using scanning electron microscopy (SEM) (Philips FEI XL30). Particles with a polydispersity index (PDI) of less than 10% were used in subsequent steps. Reaction of the silica core nanoparticles with (3-aminopropyl) triethoxysilane (APTES, Sigma-Aldrich) provided amine groups on the surface of the core to allow for deposition of gold colloid. Gold colloid was prepared to a size of 2–4 nm in the method of Duff et al. and aged 2–3 weeks at 4 °C [42]. The colloid was then concentrated 20X through rotary evaporation and mixed with the aminated silica particles that facilitated the formation of gold nucleation sites in the subsequent reduction of gold from $HAuCl_4$ in the presence of formaldehyde. The reduction of gold around the initial colloid sites enabled the formation of gold islands that coalesced to form a contiguous gold shell. The extinction characteristics of the nanoshells were determined using a UV–Vis spectrophotometer (Carey 50 Varian, Walnut Creek, CA). MIE theory simulations based on previously published results and measured dimensions of the nanoshells were used to determine the extinction coefficients of the particles from which the concentration of the nanoshell suspension was calculated [27].

2.2. Hydrogel fabrication

Prior to use, NIPAAm was dissolved in THF and recrystallized in *n*-hexane so as to remove the *p*-methoxylphenol inhibitor. A molar ratio of 95:5 (NIPAAm:AAm), which has been previously shown to produce an LCST of ~40 °C was used to fabricate nanoshell-composite hydrogels by first adding 3.56 mL NIPAAm (1.75 M), 21.88 μL AAm (15 M), 51.78 μL

MBAAm (0.169 M), and varying concentrations of SiO_2–Au nanoshells (2×10^9, 4×10^9, and 6×10^9 nanoshells/mL) to a three-neck round bottom flask with stirring to form the primary polymer solution [40,43]. The MBAAm was added as the crosslinker at a molar ratio of 1/750 (crosslinker/monomer) as previously described [26]. Argon (Ar) gas was then bubbled through the primary solution for 20 min to remove dissolved O_2 in the reaction mixture. With stirring, 37.5 μL of 10% APS (w/v) and 7.5 μL TEMED were then simultaneously added to the flask in order to initiate the redox reaction for free radical polymerization of the hydrogel. The hydrogel reaction solution was then quickly poured into a glass mold that consisted of two glass slides separated by 1.5 mm Teflon® spacers, which were held together with metal clamps. The mold was then incubated at 30 °C for 2 h in a vacuum oven purged with Ar (g) to cure the hydrogel. After curing, 0.7 cm disks were punched out with a cork borer and transferred to a dish with 95% ethanol to remove organic solvents. The alcohol was changed every 4 h over a 24 h period. After 24 h, the hydrogel disks were then transferred to a dish with ultrapure water to remove unreacted reactants. The water was changed every 5 h for 3 d. The hydrogel disks were dried over P_2O_5 overnight and transferred to a vacuum oven to be completely dried. Control hydrogels without nanoshells were fabricated using the same method without the addition of the nanoshells to the primary monomer solution.

2.3. Thermal behavior of nanoshell-composite hydrogels

Dried composite hydrogels of varying nanoshell concentrations were weighed and transferred to Coulter counter vials and swelled in 4.0 mL of Tris buffer (0.05 M, pH 7.4) for 24 h at room temperature. After 24 h, the hydrogels were weighed and the vials containing the gels were transferred to a 50 °C water bath for 80 min, during which the weights of the hydrogels were recorded at 10 min intervals. Prior to being weighed, the hydrogels were briefly dabbed with a damp Kimwipe to remove excess surface water. The deswelling ratios (DSR) of the hydrogels were then calculated ($DSR = W_t / W_{t=0}$ where W_t and $W_{t=0}$ are the weight of the swollen hydrogel at a predetermined time and weight at a time point of 0 min respectively).

2.4. Reversible thermal behavior of nanoshell-composite hydrogels

To determine the reversible thermal behavior of the composite hydrogels, dried composite hydrogels of varying nanoshell concentrations were weighed and swelled in Tris buffer as described above and the dry and wet weight of each disk was recorded. The vials containing the hydrogels were transferred to a 50 °C water bath for 180 min and the weight of each gel was determined at predetermined time intervals. After 180 min, the disks were then moved to room temperature vials containing 4.0 mL of buffer and the weights of the hydrogels were determined at 190, 200, 210, 220, 230, 240, 260, 280, 300, 320, 340, and 360 min. The hydrogels were then reswelled at room temperature overnight and the process of deswelling followed by reswelling was repeated for the same samples over a 3 d period, in which the weights of the gels were recorded at predetermined time intervals. The deswelling ratios of the hydrogels were then determined as described above.

2.5. Photothermal behavior of nanoshell-composite hydrogels

To determine the photothermal behavior of composite hydrogels of varying nanoshell concentrations as well as different laser fluences (1.0 W/cm^2, 1.3 W/cm^2, and 1.6 W/cm^2) after irradiation, dried hydrogels were weighed and swelled in Tris buffer as previously described. The hydrogels were then transferred to wells of a 6-well tissue culture dish that contained 4 mL of fresh Tris buffer. Each hydrogel was then irradiated for 80 min along its vertical axis with a NIR laser using an Integrated Fiber Array Packet, FAP-I System, with a wavelength of 808 nm (Coherent, Santa Clara, CA) so that the entire hydrogel was within the cross-sectional area of the beam. During the irradiation time, the hydrogel was quickly removed, dabbed with a Kimwipe as described above, and weighed at predetermined time intervals. Following irradiation, the hydrogels were reswelled at room temperature for 160 min, during which the weights of the hydrogels were recorded at predetermined time intervals. The deswelling ratios of the hydrogels were determined as described above. The results showed that maximum deswelling of the composite hydrogels occurred at laser fluences greater than 1.0 W/cm^2, which was independent of the nanoshell concentration. Thus, subsequent studies were performed with composite hydrogels containing 2×10^9 nanoshells/mL at a laser fluence of 1.3 W/cm^2.

2.6. Reversible photothermal behavior of nanoshell-composite hydrogels

To determine the reversible photothermal behavior of the composite hydrogels, dried hydrogels containing 2×10^9 nanoshells/mL were weighed and swelled in Tris buffer as described above. The wet weights of the hydrogels were recorded and the gels were then transferred to the wells of a 6-well tissue culture plate that contained 4.0 mL of Tris buffer. The hydrogels were then completely collapsed by exposure to the laser for 30 min at 1.3 W/cm^2 and the weights of the hydrogels were recorded. The hydrogels were then reswelled for 1 h, during which the weights of the hydrogels were recorded every 20 min. After 1 h, the hydrogels were then irradiated for 10 min, during which the hydrogels were weighed at 5 min intervals and this procedure was then repeated three times. The deswelling ratios as a function of time was then calculated as described above.

2.7. Photothermal modulated drug release

Dried nanoshell-composite hydrogels containing 2×10^9 nanoshells/mL and controls were weighed and transferred to Coulter counter vials containing 0.33 mg/mL solutions of methylene blue (MW 374) and allowed to swell for 48 h at 4 °C. Prior to irradiation, the hydrogels were quickly rinsed in 0.05 M Tris buffer, transferred to wells of a 6-well tissue culture plate, which contained 4 mL of fresh Tris buffer, and irradiated at a

laser fluence of 1.3 W/cm^2 for 60 min as described above. During irradiation, 60 μL samples were removed from the wells at predetermined time intervals and stored at −20 °C for analysis. The absorbance of the samples was determined at 664 nm from which the concentration of methylene blue in the release buffer was determined.

Dried nanoshell-composite hydrogels containing 2×10^9 nanoshells/mL and controls were weighed and transferred to Coulter counter vials containing 10 mg/mL solutions of insulin (MW 5, 800) or lysozyme (MW 14, 700) and allowed to swell for 48 h at 4 °C. Prior to irradiation, the hydrogels were quickly rinsed in 0.05 M Tris buffer, transferred to wells of a 6-well tissue culture plate, which contained 4 mL of fresh Tris buffer, and irradiated at a laser fluence of 1.3 W/cm^2 for 60 min as described above. During irradiation, 60 μL samples were removed from the wells at predetermined time intervals and stored at −20 °C for analysis. The amount of released protein was determined using the BCA protein assay.

2.8. Characterization of released protein

In order to verify that there was no degradation of the protein released from the delivery system upon irradiation of the hydrogel, samples of protein released from the experiment outlined above were run on an SDS-PAGE gel to verify the molecular weights of the released protein.

2.8.1. SDS-PAGE and silver staining

To verify that the molecular weight of the released protein from the irradiated nanoshell-composite hydrogels was identical to that of the control protein, 25 ng samples of insulin and lysozyme obtained above were separated by sodium dodecyl sulfate-polyacrylamide gel electrophoresis (SDS-PAGE) followed by silver staining for detection of protein. Briefly, protein samples were denatured in sample buffer (0.5 M Tris–HCl, pH 6.8, 10% (w/v) sodium dodecyl sulfate, 25% glycerol, 0.5% (w/v) bromophenol blue, and 5% (v/v) β-mercaptoethanol that was then heated to 95 °C for 4 min. The samples were cooled on ice and the proteins were separated on a Ready gel Tris–HCl gel (4–15% linear gradient) under denaturing conditions. The gel was then silver stained for detection of protein with a Bio-rad silver stain plus kit as per manufacturer's instructions.

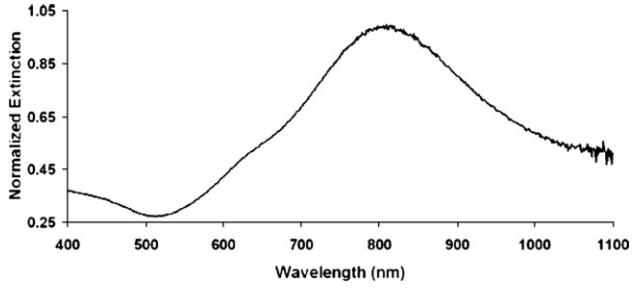

Fig. 1. The normalized extinction spectrum of fabricated SiO_2–Au nanoshells with peak at 804 nm.

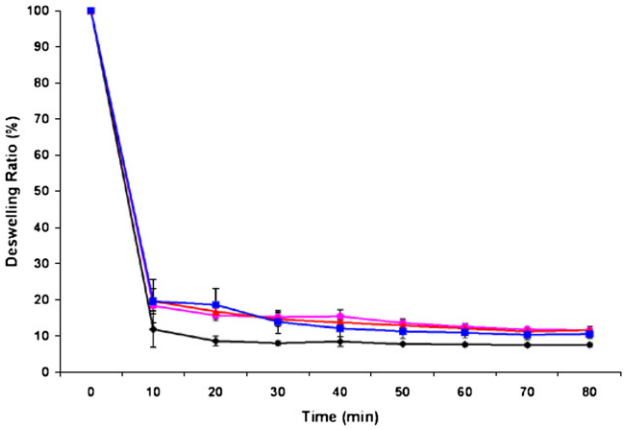

Fig. 2. Thermal deswelling of NIPAAm-*co*-AAm control hydrogels (diamond) and nanoshell-composite hydrogels with varying concentrations of SiO_2–Au nanoshells (circle=2×10^9 nanoshells/mL; triangle=4×10^9 nanoshells/mL; square=6×10^9 nanoshells/mL) at 50 °C as a function of time. Data reported as mean±SD, $n=3$.

2.8.2. Statistics

Statistical analysis was performed with Graph-Pad Prism® version 3.02 software using one-way ANOVA with Tukey's post-hoc test for p-values ≤ 0.05. Data represented with error bars indicate sample group mean±standard deviation of the mean (σ).

3. Results

3.1. Characterization of SiO_2–Au nanoshells

The nanoshells were made with silica cores of 119±11 nm in diameter and the shell thickness was calculated to be 14 nm, which produced SiO_2–Au nanoshells with a particle size of 146 nm. The measured extinction spectra of the nanoshells used in this study exhibited a peak at ~804 nm (Fig. 1).

3.2. Thermal deswelling

The ability of the composite hydrogels to completely collapse at 50 °C despite the presence of SiO_2–Au nanoshells was investigated and the degree of collapse was reported as the deswelling ratios. As can be seen from the thermal behavior of the nanoshell-composite hydrogels, deswelling of the composite hydrogels occurred rapidly within 10 min of being immersed in the 50 °C water bath, which was consistent with the NIPAAm-*co*-AAm control hydrogels (Fig. 2). The average deswelling ratio for the composite hydrogels with different nanoshell concentrations after 10 min incubation was ~19.2±3.3% compared with 11.9±5.1% for the control hydrogels ($p>0.05$). Complete deswelling of the composite hydrogels was achieved after 30 min in which the composite hydrogels of varying nanoshell concentrations had an average deswelling ratio of ~14.6±2.2% compared with 8.0±0.7% for the control hydrogels ($p<0.01$).

3.3. Reversible thermal deswelling

To determine whether the deswelling ratios of the composite hydrogels were reversible after complete collapse, the hydrogels

were reswollen at room temperature and collapsed repeatedly over time. The data show that the nanoshell-composite hydrogels were able to reswell to their original weights at room temperature, at the same rate as that of the NIPAAm-*co*-AAm control hydrogels (Fig. 3). Repeated collapse of the composite hydrogels at 50 °C after the gels were reswollen at room temperature showed that the collapse and thus the deswelling ratios of the composite hydrogels were reversible and comparable to the control hydrogels.

3.4. Photothermal deswelling

To investigate whether irradiation of the SiO_2–Au nanoshells within the temperature-sensitive hydrogel can induce collapse of the hydrogels, nanoshell-composite hydrogels with varying concentrations of nanoshells were irradiated at three different laser fluences. The data showed that irradiation of the composite hydrogels with the NIR laser resulted in rapid collapse of the hydrogels as a function of time. At a low laser power of 1.0 W/cm^2, the composite hydrogels showed maximum deswelling ratios of 35.9±12.0%, 21.3±9.0%, and 14.6±0.4% after 80 min of irradiation for the nanoshell-composite hydrogels that contained 2×10^9, 4×10^9, and 6×10^9 nanoshells/mL respectively (Fig. 4A). At laser fluences above 1.0 W/cm^2, all nanoshell-composite hydrogels showed maximum deswelling ratios of ~15% after 80 min of laser irradiation, which was independent of the nanoshell concentration (Fig. 4B and C). In contrast, NIPAAm-*co*-AAm control hydrogels showed negligible deswelling ratios after 80 min of irradiation (Fig. 4).

3.5. Reversible photothermal deswelling

In order to investigate the reversibility and repeatability of the laser-induced collapse of the nanoshell-composite hydrogels, hydrogels with 2×10^9 nanoshells/mL were repeatedly irradiated and reswelled at room temperature as a function of time. The data showed that irradiation of the SiO_2–Au nanoshell-composite hydrogels resulted in rapid collapse of the hydrogels within 30 min, which was followed by complete reswelling of the hydrogels at room temperature (Fig. 5).

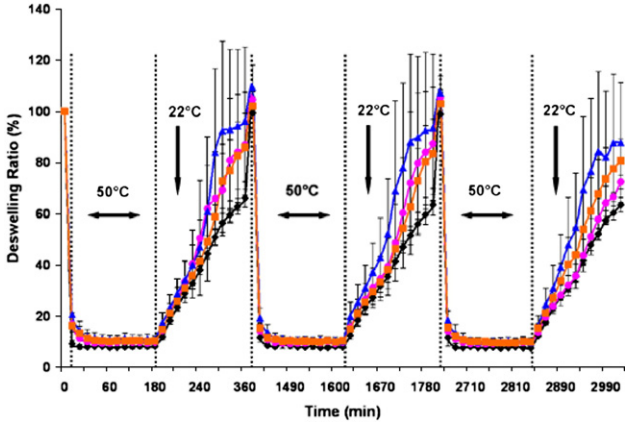

Fig. 3. Reversible thermal behavior of NIPAAm-*co*-AAm control hydrogels (diamond) and nanoshell-composite hydrogels with varying concentrations of SiO_2–Au nanoshells (circle=2×10^9 nanoshells/mL; triangle=4×10^9 nanoshells/mL; square=6×10^9 nanoshells/mL) showing reversible collapse of the hydrogels at 50 °C followed by hydrogel reswelling at 20 °C as a function of time. Data reported as mean±SD, n=3.

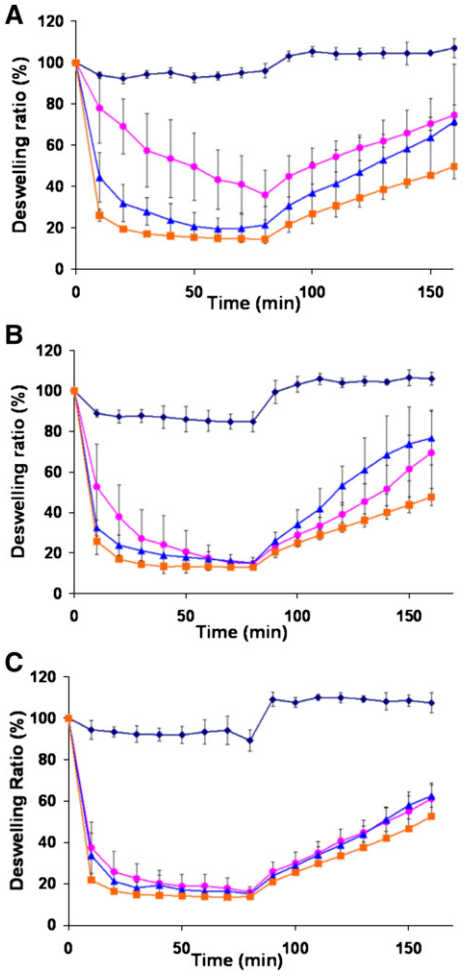

Fig. 4. Photothermal behavior of NIPAAm-*co*-AAm control hydrogels (diamond) and nanoshell-composite hydrogels with varying concentrations of SiO_2–Au nanoshells (circle=2×10^9 nanoshells/mL; triangle=4×10^9 nanoshells/mL; square=6×10^9 nanoshells/mL) showing rapid collapse of the hydrogels at 1.0 W/cm^2 (A), 1.3 W/cm^2 (B), and 1.6 W/cm^2 (C) during laser irradiation followed by reswelling after irradiation as a function of time. Data reported as mean±SD, n=3.

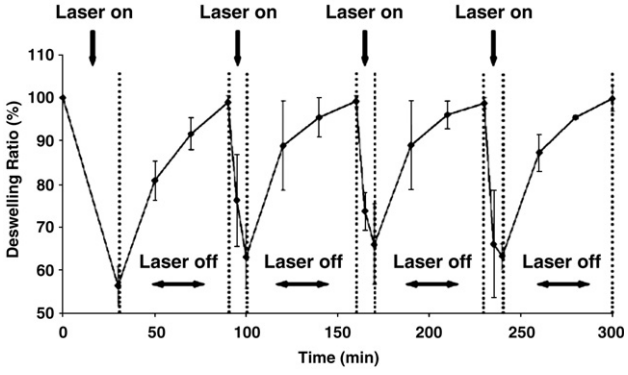

Fig. 5. Reversible photothermal behavior of composite hydrogels with 2×10^9 nanoshells/mL showing collapse and reswelling of the hydrogels during and after laser irradiation as a function of time. Data reported as mean±SD, n=3.

Repeated irradiation of the nanoshell-composite hydrogels resulted in completely reversible collapse and reswelling over time. In addition, the rate of collapse and reswelling of the nanoshell-composite hydrogels were consistent with that of the control NIPAAm-*co*-AAm hydrogels.

3.6. Photothermal modulated drug release

The release of the model drug methylene blue from the nanoshell-composite hydrogels occurred spontaneously prior to irradiation of the hydrogel in which ~14.1 mg of methylene blue/g of polymer dry weight (mg/g dry weight) was released (Fig. 6). However, after irradiation of the nanoshell-composite hydrogels there was a significant increase in the amount of methylene blue released upon laser irradiation (23.2±2.98 and 24.5±3.58 mg/g dry weight) compared to the control irradiated hydrogels (13.8±1.68 and 15.7±1.66 mg/g dry weight) without nanoshells at times 18 and 24.5 min respectively ($p<0.05$). Further irradiation of the hydrogels resulted in similar levels of methylene blue released from both the nanoshell-composite hydrogels as well as the hydrogels without nanoshells ($p>0.05$).

Irradiation of nanoshell-composite hydrogels preswelled in the insulin solution resulted in a burst release of insulin in which ~2 times as much insulin was released from the irradiated composite hydrogels compared to the irradiated control without the nanoshells at times 18 and 24.5 min respectively ($p<0.05$) (Fig. 7). Further irradiation of the nanoshell-composite hydrogels resulted in significantly higher amount of insulin released (17.9±2.61 and 21.9±1.50 mg/g dry weight) compared to the control irradiated hydrogels (12.9±2.02 and 13.2±2.75 mg/g dry weight) without nanoshells at times 41 and 57.5 min respectively ($p<0.05$). Analysis of the protein released from the irradiated nanoshell-composite hydrogel after 57.5 min showed that the released insulin protein had the same molecular weight as the insulin control without any degradation observed (Fig. 7, inset).

The release of the lysozyme protein from nanoshell-composite hydrogels occurred only upon laser irradiation that resulted in a burst release of lysozyme in which there was ~8 times more lysozyme released from the irradiated composite hydrogels compared to the irradiated control without the nanoshells at times 18 and 24.5 min respectively ($p=0.01$) (Fig. 8). Additional irradiation of the nanoshell-composite hydrogels resulted in significantly higher amount of lysozyme released (32.8±1.86 and 34.7±7.37 mg/g dry weight) compared to the control irradiated hydrogels (8.28±4.53 and 9.02±5.06 mg/g dry weight) without nanoshells at times 41 and 57.5 min respectively ($p=0.01$). Analysis of the lysozyme protein released from the irradiated nanoshell-composite hydrogel after 57.5 min showed that the released lysozyme protein had the same molecular weight as the lysozyme control without any degradation observed (Fig. 8, inset).

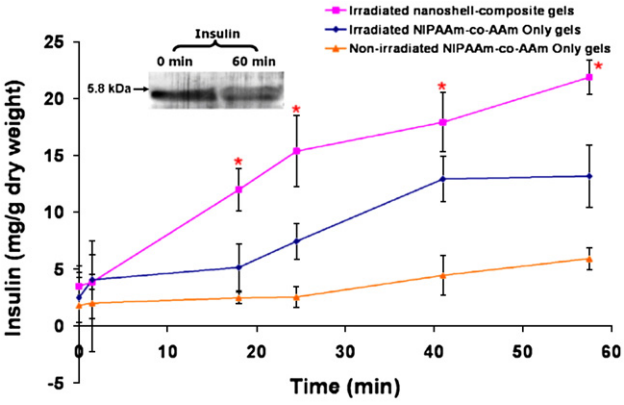

Fig. 7. Release of insulin (mg/g dry weight represents mg of insulin released/g of polymer dry weight) from irradiated nanoshell-composite hydrogels (square), irradiated NIPAAm-*co*-AAm hydrogels (diamond), and nonirradiated NIPAAm-*co*-AAm hydrogels (triangle) as a function of time. SDS-PAGE gel for insulin control taken from protein solution used to swell hydrogels (0 min) and for insulin released after 60 min laser irradiation (60 min). Data reported as mean± SD, $n=3$.

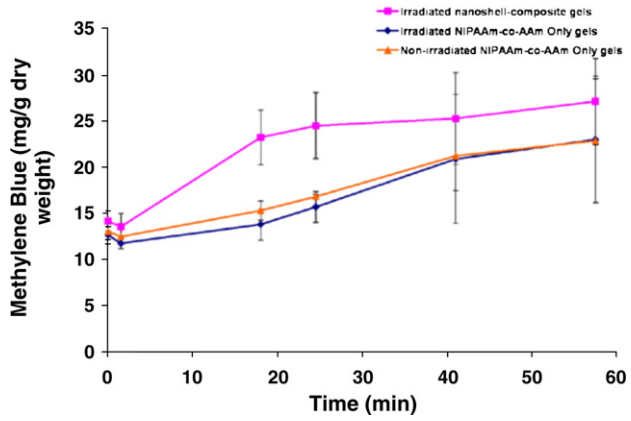

Fig. 6. Release of methylene blue (mg/g dry weight represents mg of methylene blue released/g of polymer dry weight) from irradiated nanoshell-composite hydrogels (square), irradiated NIPAAm-*co*-AAm hydrogels (diamond), and nonirradiated NIPAAm-*co*-AAm hydrogels (triangle) as a function of time. Data reported as mean±SD, $n=3$.

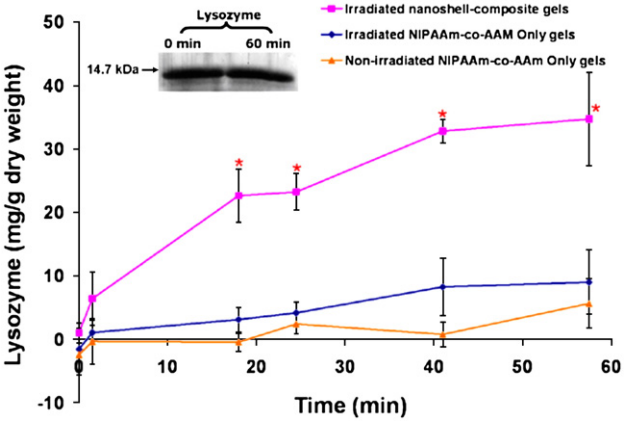

Fig. 8. Release of lysozyme (mg/g dry weight represents mg of lysozyme released/g of polymer dry weight) from irradiated nanoshell-composite hydrogels (square), irradiated NIPAAm-*co*-AAm hydrogels (diamond), and nonirradiated NIPAAm-*co*-AAm hydrogels (triangle) as a function of time. SDS-PAGE gel for lysozyme control taken from protein solution used to swell hydrogels (0 min) and for lysozyme released after 60 min laser irradiation (60 min). Data reported as mean±SD, $n=3$.

4. Discussion

In the field of drug delivery, modulated release of a therapeutic molecule or protein in a pulsatile or staggered manner in response to physiological requirements remains a hurdle that needs to be overcome. These systems that respond to physiological requirements are highly suitable for the release of therapeutics that are derived from non-constant plasma concentrations such as in the case of *diabetes mellitus* where only a baseline release of the drug is required following the ingestion of food [44,45]. Towards the goal of developing modulated drug delivery devices there have been many systems designed to respond to stimuli in the local environment including ultrasound [46,47], electric fields [48,49], and mechanical forces [23,50]. In the case of implantable devices, one of the limitations of the system is ready access to the device that will enable efficient release of the therapeutic drug. To this end, we have developed a stimuli-sensitive drug delivery system composed of the temperature-sensitive copolymer *N*-isopropylacrylamide (NIPAAm)-*co*-acrylamide (AAm) and silica–gold (SiO_2–Au) nanoshells for the controlled release of therapeutic drug molecules. The inclusion of nanoshells within the temperature-sensitive polymer resulted in a composite material that collapsed in response to near infrared irradiation at a wavelength that can facilitate deep tissue penetration but does not cause damage to human tissue [51,52].

In this study, we have demonstrated photothermal modulated drug delivery based on temperature-sensitive polymers and optically active nanoparticles. The SiO_2–Au nanoshells were specifically designed to strongly absorb light emitted by a diode laser (808 nm) and to convert it to heat, causing the local temperature of the nanoshell-composite hydrogels to increase rapidly upon near IR irradiation. Measurements of the peak extinction spectrum of the fabricated SiO_2–Au nanoshells showed that the particles had a peak that was almost identical to that of the laser (804 nm), which facilitated maximum irradiation of the nanoshells within the composite hydrogels (Fig. 1).

Subsequent fabrication of the temperature-sensitive nanoshell-composite hydrogels resulted in the formation of a composite material in which the inclusion of the SiO_2–Au nanoshells did not affect the deswelling properties of the NIPAAm-*co*-AAm copolymers after immersion of the hydrogels in the 50 °C water bath (Fig. 2). In addition, even though there was no difference in the degree of deswelling observed for the composite hydrogels of varying concentrations of SiO_2–Au nanoshells, there was a significant difference in the deswelling ratio of the NIPAAm-*co*-AAm control that may be due to the formation of the composite material in which the presence of the nanoshells prevent complete collapse that was observed for the composite material. Moreover, the presence of the SiO_2–Au nanoshells did not affect the reversible collapse of the NIPAAm-*co*-AAm copolymers in which complete reswelling of the hydrogels after collapse in the 50 °C water bath was observed upon incubation of the gels at room temperature (Fig. 3). Thus, the completely reversible and repeatable collapse of the hydrogels showed that the fabrication of the hydrogels with nanoshells did not affect the physical property of the copolymers.

The ability of the nanoshell-composite hydrogels to collapse upon irradiation of the gels with the NIR laser showed that the degree of deswelling of the composite hydrogels could be controlled with different nanoshell concentrations as well as with different fluences of the laser. At the lowest laser fluence of 1.0 W/cm^2, the degree of deswelling of the hydrogel could be limited with the lowest concentration of SiO_2–Au nanoshells that produce a maximum deswelling ratio of ~35% for the composite hydrogels containing 2×10^9 nanoshells/mL compared to ~21% and 15% for the composite hydrogels containing 4×10^9 nanoshells/mL and 6×10^9 nanoshells/mL after 80 min of laser irradiation respectively (Fig. 4A). In contrast, at higher laser fluences there was no difference in the degree of deswelling of the composite hydrogels after irradiation of the nanoshell-composite hydrogels, which showed that there was a saturation limit obtained with nanoshell concentrations above 2×10^9 nanoshells/mL (Fig. 4B and C). In addition, the laser-induced deswelling of the nanoshell-composite hydrogels was found to be completely reversible and repeatable after the laser was turned off and the hydrogels were allowed to reswell (Fig. 5).

The NIR laser-induced collapse of the nanoshell-composite hydrogels was used for modulated drug release of methylene blue, insulin, and lysozyme. The data showed that there was little control of methylene blue release from the composite hydrogels as shown by the spontaneous release of the model drug from the hydrogel at time 0 despite no irradiation (Fig. 6). Moreover, even though there were higher amounts of the model drug released at times 18 and 24.5 min from the composite hydrogels compared to the hydrogels without nanoshells the data indicated that the low molecular weight model drug was small enough to diffuse freely from the hydrogel in which the pore size and the tortuosity of the hydrogel does not provide a larger barrier to the diffusion of methylene blue. Thus, the higher amounts of drug release were probably due to a combination of convective forces of the drug out of the hydrogel due to physical collapse of the hydrogel upon irradiation as well as to diffusive forces. However, eventually over time the diffusive forces of the model drug can overcome the effects of convective forces and hence similar amounts of the drug were released from both systems.

The data for the photothermal modulated release of insulin from the nanoshell-composite hydrogels showed that the pore size and tortuosity of the hydrogel have become significant barriers to the diffusion of the higher molecular weight protein such that there was significantly less diffusion of insulin out of the hydrogel compared to the irradiated gels (Fig. 7). Therefore, convective transport of insulin has become the driving force of the drug out of the hydrogel. In addition, the SDS-PAGE gel showed that there was no degradation of the released protein and that the molecular weight of the protein was identical to the control insulin, which suggests that the biological property of the released protein may be intact. Future studies will be focused on analyzing the biological efficacy of the released insulin.

The release profile for the modulated release of lysozyme from the nanoshell-composite hydrogels showed that significant amounts of the higher molecular weight protein was only released upon irradiation of the hydrogels. Thus, the data indicates that convective forces are the predominant driving force for lysozyme and that the pore size of the hydrogel has become a more significant barrier to diffusion of the protein

compared to insulin. Therefore, the cumulative drug release data suggest that there is a molecular weight cutoff for the release of therapeutic drugs out of the hydrogel. In fact controlled drug release studies with bovine serum albumin (BSA) did not show any release of the protein from the hydrogels, which suggested that the molecular weight of BSA was too large to pass through the hydrogel pores (data not shown). The crosslink density of the nanoshell-composite hydrogels determines the size of the molecules that can be released from this system. In order to accommodate smaller molecular weight compounds, the cross-link density can be increased in order to reduce diffusion of the drug out of the hydrogel. In addition, the SDS-PAGE gel for lysozyme also showed that there was no degradation of the released protein and that the molecular weight of the protein was identical to the control insulin that indicates that controlled release of proteins from these temperature-sensitive composite hydrogels may be suitable drug delivery devices for therapeutic proteins.

The system described in this paper demonstrates the ability to switch between a passive, diffusional rate of drug delivery and an active, accelerated rate in response to near infrared irradiation. It has the potential to provide a simple, minimally invasive alternative to serial injections when repetitive dosing is required. Additionally, altering the irradiation parameters, hydrogel composition, and loading methods can allow us to match the release profile of a drug to the requirements of an individual treatment. Thus, the capacity to deliver an increased amount of drug to a patient in response to an external signal may prove useful in disease states where an intricate dosing regimen is desired, such as diabetes mellitus, many cardiovascular diseases, and some forms of cancer.

5. Conclusions

In this present work, a new class of silica–gold nanoshells of varying concentrations was successfully embedded within temperature-sensitive hydrogels to develop a photothermal modulated drug delivery system. These optically active nanoshells were specifically designed to absorb NIR light corresponding to the diode laser used in the experiments that facilitated maximum irradiation of the nanoshells. Subsequent irradiation of nanoshell-composite hydrogels resulted in varying degrees of collapse of the hydrogels as a function of the nanoshell concentration as well as the laser fluence. In addition, the release profiles of embedded drugs from the hydrogels upon laser irradiation were found to be dependent upon the molecular weight of the therapeutic molecules. Thus, these new nanoshell-composite hydrogels have potential applications in many diseases that only require the release of a drug in response to metabolic requirements.

Acknowledgements

This work was supported by the National Science Foundation (NSF) Nanoscale Science and Engineering Center for Biological and Environmental Nanotechnology, Award Number EEC-0118007.

References

[1] Z. Wu, Y. Jiang, T. Kim, K. Lee, Effects of surface coating on the controlled release of vitamin B1 from mesoporous silica tablets, J. Control. Release 119 (2007) 215–221.
[2] M.M. Arnold, E.M. Gorman, L.J. Schieber, E.J. Munson, C. Berkland, NanoCipro encapsulation in monodisperse large porous PLGA microparticles, J. Control. Release 121 (2007) 100–109.
[3] K.J. Robertson, E. Schoenle, Z. Gucev, L. Mordhorst, M.A. Gall, J. Ludvigsson, Insulin detemir compared with NPH insulin in children and adolescents with Type 1 diabetes, Diabet. Med. 24 (2007) 27–34.
[4] H. Smulyan, Nitrates, arterial function, wave reflections and coronary heart disease, Adv. Cardiol. 44 (2007) 302–314.
[5] J. Malm, G.J. Grover, M. Farnegardh, Recent advances in the development of agonists selective for beta1-type thyroid hormone receptor, Mini. Rev. Med. Chem. 7 (2007) 79–86.
[6] F. Fischel-Ghodsian, L. Brown, E. Mathiowitz, D. Brandenburg, R. Langer, Enzymatically controlled drug delivery, Proc. Natl. Acad. Sci. U. S. A. 85 (1988) 2403–2406.
[7] M. Tang, R. Zhang, A. Bowyer, R. Eisenthal, J. Hubble, A reversible hydrogel membrane for controlling the delivery of macromolecules, Biotechnol. Bioeng. 82 (2003) 47–53.
[8] A. Matsumoto, R. Yoshida, K. Kataoka, Glucose-responsive polymer gel bearing phenylborate derivative as a glucose-sensing moiety operating at the physiological pH, Biomacromolecules 5 (2004) 1038–1045.
[9] S.H. Hu, T.Y. Liu, D.M. Liu, S.Y. Chen, Nano-ferrosponges for controlled drug release, J. Control. Release 121 (3) (2007) 181–189.
[10] A.S. Lubbe, C. Bergemann, W. Huhnt, T. Fricke, H. Riess, J.W. Brock, D. Huhn, Preclinical experiences with magnetic drug targeting: tolerance and efficacy, Cancer Res. 56 (1996) 4694–4701.
[11] A.F. Lum, M.A. Borden, P.A. Dayton, D.E. Kruse, S.I. Simon, K.W. Ferrara, Ultrasound radiation force enables targeted deposition of model drug carriers loaded on microbubbles, J. Control. Release 111 (2006) 128–134.
[12] S. Miyazaki, C. Yokouchi, M. Takada, External control of drug release: controlled release of insulin from a hydrophilic polymer implant by ultrasound irradiation in diabetic rats, J. Pharm. Pharmacol. 40 (1988) 716–717.
[13] T. Terahara, S. Mitragotri, J. Kost, R. Langer, Dependence of low-frequency sonophoresis on ultrasound parameters; distance of the horn and intensity, Int. J. Pharm. 235 (2002) 35–42.
[14] J.B. Davies, V.T. Ciavatta, J.H. Boatright, J.M. Nickerson, Delivery of several forms of DNA, DNA–RNA hybrids, and dyes across human sclera by electrical fields, Mol. Vis. 9 (2003) 569–578.
[15] I.C. Kwon, Y.H. Bae, S.W. Kim, Electrically erodible polymer gel for controlled release of drugs, Nature 354 (1991) 291–293.
[16] F.M. Chen, Y.M. Zhao, H.H. Sun, T. Jin, Q.T. Wang, W. Zhou, Z.F. Wu, Y. Jin, Novel glycidyl methacrylated dextran (Dex-GMA)/gelatin hydrogel scaffolds containing microspheres loaded with bone morphogenetic proteins: formulation and characteristics, J. Control. Release 118 (2007) 65–77.
[17] Y. Liu, W.L. Lu, J.C. Wang, X. Zhang, H. Zhang, X.Q. Wang, T.Y. Zhou, Q. Zhang, Controlled delivery of recombinant hirudin based on thermo-sensitive Pluronic F127 hydrogel for subcutaneous administration: in vitro and in vivo characterization, J. Control. Release 117 (2007) 387–395.
[18] Y. Yamamoto, K. Yasugi, A. Harada, Y. Nagasaki, K. Kataoka, Temperature-related change in the properties relevant to drug delivery of poly(ethylene glycol)-poly(D,L-lactide) block copolymer micelles in aqueous milieu, J. Control. Release 82 (2002) 359–371.
[19] S. Jo, J. Kim, S.W. Kim, Reverse thermal gelation of aliphatically modified biodegradable triblock copolymers, Macromol. Biosci. 6 (2006) 923–928.
[20] V.A. Sethuraman, Y.H. Bae, TAT peptide-based micelle system for potential active targeting of anti-cancer agents to acidic solid tumors, J. Control. Release 118 (2) (2006) 216–224.
[21] R. Jayakumar, R.L. Reis, J.F. Mano, Synthesis and characterization of pH-sensitive thiol-containing chitosan beads for controlled drug delivery applications, Drug Deliv. 14 (2007) 9–17.
[22] K.Y. Lee, M.C. Peters, K.W. Anderson, D.J. Mooney, Controlled growth factor release from synthetic extracellular matrices, Nature 408 (2000) 998–1000.

[23] J.H. Park, M.G. Allen, M.R. Prausnitz, Biodegradable polymer microneedles: fabrication, mechanics and transdermal drug delivery, J. Control. Release 104 (2005) 51–66.
[24] A. Mamada, T. Tanaka, D. Kungwachakun, M. Irie, Photo-induced phase transition of gels, Macromolecules 23 (1990) 1517–1519.
[25] A. Suzuki, T. Tanaka, Phase transition in polymer gels induced by visible light, Nature 346 (1990) 345–347.
[26] S.R. Sershen, S.L. Westcott, N.J. Halas, J.L. West, Temperature-sensitive polymer-nanoshell composites for photothermally modulated drug delivery, J. Biomed. Mater. Res. 51 (2000) 293–298.
[27] R.D. Averitt, S.L. Westcott, N.J. Halas, Linear optical properties of gold nanoshells, J. Opt. Soc. Am. B. 16 (1999) 1824–1832.
[28] S.J. Oldenburg, R.D. Averitt, S.L. Westcott, N.J. Nalas, Nanoengineering of optical resonances, Chem. Phys. Lett. 288 (1998) 243–247.
[29] S.J. Oldenburg, J.B. Jackson, S.L. Westcott, N.J. Halas, Infrared extinction properties of gold nanoshells, Appl. Phys. Lett. 75 (1999) 2897–2899.
[30] L.R. Hirsch, J.B. Jackson, A. Lee, N.J. Halas, J.L. West, A whole blood immunoassay using gold nanoshells, Anal. Chem. 75 (2003) 2377–2381.
[31] C. Loo, A. Lowery, N.J. Halas, J.L. West, R. Drezek, Immunotargeted nanoshells for integrated cancer imaging and therapy, Nano Lett. 5 (2005) 709–711.
[32] C. Loo, L. Hirsch, M.H. Lee, E. Chang, J. West, N. Halas, R. Drezek, Gold nanoshell bioconjugates for molecular imaging in living cells, Opt. Lett. 30 (2005) 1012–1014.
[33] A.M. Gobin, D.P. O'Neal, D.M. Watkins, N.J. Halas, R.A. Drezek, J.L. West, Near infrared laser-tissue welding using nanoshells as an exogenous absorber, Lasers Surg. Med. 37 (2005) 123–129.
[34] M. Sutter, J. Siepmann, W.E. Hennink, W. Jiskoot, Recombinant gelatin hydrogels for the sustained release of proteins, J. Control. Release 119 (2007) 301–312.
[35] K. Hori, C. Sotozono, J. Hamuro, K. Yamasaki, Y. Kimura, M. Ozeki, Y. Tabata, S. Kinoshita, Controlled-release of epidermal growth factor from cationized gelatin hydrogel enhances corneal epithelial wound healing, J. Control. Release 118 (2007) 169–176.
[36] R. Yoshida, K. Sakai, T. Okano, Y. Sakurai, Modulating the phase transition temperature and thermosensitivity in *N*-isopropylacrylamide copolymer gels, J. Biomater. Sci., Polym. Ed. 6 (1994) 585–598.
[37] J.Y. Wu, S.Q. Liu, P.W. Heng, Y.Y. Yang, Evaluating proteins release from, and their interactions with, thermosensitive poly (*N*-isopropylacrylamide) hydrogels, J. Control. Release 102 (2005) 361–372.
[38] D.L. Taylor, D.L. Cerankowski, Preparation of films exhibiting balanced temperature dependence to permeation by aqueous solution—a study of lower consulate behaviour, J. Polym. Sci., Polym. Chem. Ed. 13 (1975) 2551.
[39] J.H. Priest, S.L. Murray, R.J. Nelson, A.S. Hoffman, Lower critical solution temperatures of aqueous copolymers of *N*-isopropylacrylamide and other *N*-substituted acrylamides, Revers. Polym. Gels Rel. Syst. 350 (1987) 255–264.
[40] L.C. Dong, A.S. Hoffman, Swelling characteristics and activities of copoly (*N*-isopropylacrylamide-acrylamide) gels containing immobilized asparaginase, Revers. Polym. Gels Relat. Syst. 350 (1987) 236–244.
[41] W. Stober, A. Fink, Controlled growth of monodisperse silica spheres in the micron size range, J. Colloid Interface Sci. 26 (1968) 62–69.
[42] D.G. Duff, A. Baiker, P.P. Edwards, A new hydrosol of gold clusters. 1. Formation and particle size variation, Langmuir 9 (1993) 2301–2309.
[43] J.H. Priest, S.L. Murray, R.J. Nelson, A.S. Hoffman, Lower critical solution temperature of aqueous copolymers of *N*-isopropylacrylamide and other *N*-substituted acrylamides, Revers. Polym. Gels Relat. Syst. 350 (1987) 255–264.
[44] O.B. Crofford, Diabetes control and complications, Annu. Rev. Med. 46 (1995) 267–279.
[45] F.R. Kaufman, Diabetes mellitus, Pediatr. Rev. 18 (1997) 383–392.
[46] M. Pong, S. Umchid, A.J. Guarino, P.A. Lewin, J. Litniewski, A. Nowicki, S.P. Wrenn, In vitro ultrasound-mediated leakage from phospholipid vesicles, Ultrasonics 45 (2006) 133–145.
[47] Z. Gao, H.D. Fain, N. Rapoport, Ultrasound-enhanced tumor targeting of polymeric micellar drug carriers, Mol. Pharmacol. 1 (2004) 317–330.
[48] B.J. Mossop, R.C. Barr, J.W. Henshaw, D.A. Zaharoff, F. Yuan, Electric fields in tumors exposed to external voltage sources: implication for electric field-mediated drug and gene delivery, Ann. Biomed. Eng. 34 (2006) 1564–1572.
[49] M. Jensen, P. Birch Hansen, S. Murdan, S. Frokjaer, A.T. Florence, Loading into and electro-stimulated release of peptides and proteins from chondroitin 4-sulphate hydrogels, Eur. J. Pharm. Sci. 15 (2002) 139–148.
[50] J.H. Park, M.G. Allen, M.R. Prausnitz, Polymer microneedles for controlled-release drug delivery, Pharm. Res. 23 (2006) 1008–1019.
[51] D. Huang, E.A. Swanson, C.P. Lin, J.S. Schuman, W.G. Stinson, W. Chang, M.R. Hee, T. Flotte, K. Gregory, C.A. Puliafito, et al., Optical coherence tomography, Science 254 (1991) 1178–1181.
[52] A.M. Fisher, A.L. Murphree, C.J. Gomer, Clinical and preclinical photodynamic therapy, Lasers Surg. Med. 17 (1995) 2–31.